Original Article

Design of refractory SiC/ZrSi$_2$ composites: Wettability and spreading behavior of liquid Si-10Zr alloy in contact with SiC at high temperatures

Donatella Giuranno[a,b,*], Grzegorz Bruzda[b], Adelajda Polkowska[b], Rafal Nowak[b], Wojciech Polkowski[b], Artur Kudyba[b], Natalia Sobczak[b], Francesco Mocellin[a], Rada Novakovic[a]

[a] *National Research Council of Italy-Institute of Condensed Matter Chemistry and Technologies for Energy, Via De Marini 6, 16149 Genova, Italy*
[b] *Łukasiewicz Research Network-Foundry Research Institute, Zakopiańska 73 Str., 30-418 Krakow, Poland*

ARTICLE INFO

ABSTRACT

Reactive infiltration of liquid Si-enriched alloys into C- or SiC-based preforms is a viable cost-less alternative to manufacture dense and highly performant SiC-based and MMC composites.

In view to design and optimize liquid-assisted processes such as reactive infiltration, fundamental investigations on the interfacial phenomena occurring when the liquid Si-based alloys are in contact with C and SiC substrates, are crucial steps. In this context, targeted wettability studies may provide indications for predicting the key factors strongly influencing the reactive infiltration mechanisms, such as, unexpected interaction phenomena, etc. In particular, such preliminary experience may be helpful in finding the suitable set of operating conditions for fabricating tailored composites via reactive infiltration process.

Aiming to "mimic" the conventional industrial processes for manufacturing SiC/ZrSi$_2$ refractory composites, the sessile drop method was applied to study the interfacial phenomena occurring at Si-10 % atZr/SiC interfaces over the temperature range of T = 1360 °C-1450 °C.

1. Introduction

SiC-based and refractory MMC composites reinforced by high strength SiC continuous ceramic fibers or dispersed particles, emerge as ideal structural materials for several highly demanding applications, mainly in use at high temperature and exposed to aggressive environments. Under these working conditions, high strength, improved thermal shock, wear, hardness and corrosion resistance are the key requirements for the selected materials [1–5]. In particular, for advanced fission systems and even fusion reactors first wall vessels, the development of fully dense SiC-based composites, is one of the priorities [6–8].

Among the possible options under study to densify such materials, the use of a metal phase as filler for SiC/SiC$_f$, C$_f$/SiC and SiCp (SiC particles), such as transition metal silicides systems, seems really promising [6–9]. In fact, transition metal silicides are hard, chemically inert, and exhibit high electrical and thermal stability [10].

Among silicides, Zr-silicides can be considered as future structural materials for the nuclear industry. Currently, Zr-based alloys and Zr combined with Si are commonly used as cladding materials for nuclear reactors because of their ultra-high neutron capture cross sections and

long-term resistance under irradiation [11,12]. Additionally, under oxidizing/corrosive working conditions, a Zr-silicide phase evolves in a graded sandwiched of ZrO$_2$ and SiO$_2$ layers potentially protecting even under accident conditions [13].

As documented by [9], dense SiC/ZrSi$_2$ composites were successfully obtained by reactive infiltration of liquid Si-rich Si-Zr alloys into bi-modal SiC preforms without evidences of debonding phenomena or residual stress. The excellent thermo-mechanical response and corrosion resistance exhibited by the as produced composites, combined with the costless route used for their fabrication, make such materials highly competitive and marketable. Indeed, a "compact" microstructure can be easily obtained by controlling the process parameters (temperature, total pressure, porosity etc.) and promoting self-permeation of the molten phase into the SiC preform.

It is well known that a molten metal spontaneously infiltrates into porous media if the contact angle value displayed at the pore walls is significantly lower than 90°. On the other hand, the interfacial phenomena occurring at the metal/ceramic interfaces are not easy to be defined and controlled, since diffusion and reaction phenomena may concur or even compete with wettability. In a composite, these interactions may cause interfacial instability, decomposition of the

* Corresponding author at: National Research Council of Italy-Institute of Condensed Matter Chemistry and Technologies for Energy, Via De Marini 6, 16149 Genova, Italy.
E-mail address: donatella.giuranno@ge.icmate.cnr.it (D. Giuranno).

reinforcement, appearance of brittle interfacial reaction compounds, resulting in an overall decreasing of the thermo-mechanical response.

In order to make predictions and to succeed in designing and manufacturing such composites, preliminary investigations of thermo-dynamic and thermophysical properties of the melt phase, such as surface properties, density, viscosity [14–17], and in parallel, of the wetting characteristics and reactivity at the alloy/preform interfaces, emerge as crucial steps. The mentioned findings and know-how are valuable inputs for optimizing the infiltration process [18–21].

Few basic studies on liquid Si-enriched Si-Zr alloys concern calculations [22] and measurements [23] of the surface tension and fundamental wetting characteristics determination of the liquid Si-8at%Zr alloy onto (GC) glassy carbon and SiC substrates as functions of operating conditions (temperature, atmosphere) [24].

For this reason, the wettability and interaction phenomena occurring at the Si-10 at%Zr alloy/SiC (from now Si-10Zr/SiC) interface as a function of temperature were investigated both at the detected alloy melting point T = 1360 °C and at the temperature of T = 1450 °C by the sessile drop method under an inert atmosphere with reduced oxygen content and the more relevant results are presented and discussed in the present paper. Moreover, in view to define the main occurring inter-action mechanisms at the interface, wettability and spreading kinetics observed at T = 1450 °C were compared with the results obtained in the Si-10Zr alloy/Glassy Carbon system. Finally, aiming to check the re-liability of the results and procedure applied, targeted wetting experiments were performed at T = 1450 °C by dispensing the liquid Si-10Zr alloy drop onto the SiC substrate.

A careful analysis of the developed interfacial microstructures was performed by Optical and SEM/EDS microscopy techniques.

By relating the results obtained on wettability and spreading kinetics of the liquid Si-10Zr alloy in contact with SiC to the imposed operating conditions and to all the occurring interfacial phenomena driving the developed interfacial microstructure, the present work may be helpful for optimizing the infiltration process to fabricate tailored SiC-ZrSi$_2$ composites.

2. Wetting tests: experimental details

2.1. Materials and sample preparation

The Hot Pressed-SiC provided by Goodfellow© was selected as substrate material for wetting experiments, cut as plates (with a surface of 100 mm^2) and metallographically mirror polished by ultraprep diamond discs from 15 to 3 μm. The final surface finishing was achieved by diamond pastes (0.5 μm). A value of roughness Ra ≈ 1μm was measured at the SiC surface by an optical confocal-interferometric profilometer (Sensofar S-neox). A lower surface roughness equal to 20 nm was measured at the GC surface (provided by Alfa-Aesar©).

The Si-10Zr alloy samples, were prepared by mixing nominal weights of high purity Si and Zr (99.98 %-Goodfellow®) and arc melted under an Ar atmosphere (99.9999 %, O$_2$ < 0.1 ppm). The residual oxygen content inside the chamber was reduced by melting previously a Zr drop. To ensure the homogeneity of the alloy composition, the melting of every single Si-Zr sample (0,05 g) was repeated 3 times. No evidences of evaporation or material loss were revealed by checking the final weight.

The Si-Zr microstructure and composition were analysed at the cross-sectioned sample by SEM/EDS, as shown in Fig. 1. The eutectic composition detected in the bulk of alloy, was resulting with a Zr content varying from 8.15 to 9 at%. On the contrary, some ZrSi$_2$ precipitates were found embedded into the eutectic matrix at the bottom and as a layered phase segregated at the surface of the solidified drop. The presence of ZrSi$_2$ precipitates dispersed into the eutectic matrix is due to the exceeding Zr content in the alloy respect to the eutectic composition.

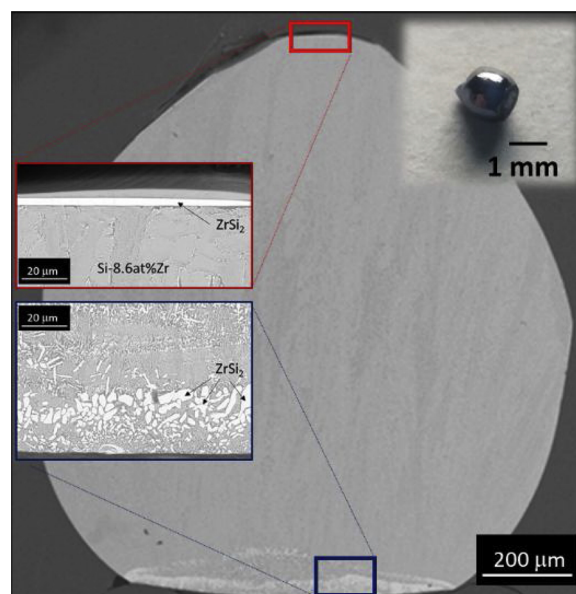Prior to the experiments, the Si-10Zr alloy sample and substrate

Fig. 1. BSE images at two magnifications and EDS analyses performed at the cross-sectioned as-produced Si-10Zr alloy sample.

were weighted, rinsed in an ultrasonic bath and dried with compressed air.

2.2. Sessile drop experiments: devices and procedures

At room temperature, the assembled Si-10Zr alloy/SiC substrate couple was placed on a graphite sample holder, located at the central part of the heater and leveled at the horizontal plane.

To remove any contaminant from the experimental environment, the device was degassed under a vacuum (P$_{tot}$ ≤ 10^{-6} mbar) for two hours.

In order to avoid evaporation and material loss, mainly at temperatures higher than the alloy melting point, the wetting tests were carried out under a static Ar atmosphere (99.9999 %, O$_2$ < 0.1 ppm) by following the procedure described elsewhere [18].

The alloy/substrate couple was heated by an 800 kHz high frequency generator coupled to a graphite tube. As detailed in [18], the presence of graphite as heating element provides an atmosphere with reduced oxygen content (PO$_2$ < 10^{-8} mbar).

Except for the wetting test performed at T = 1360 °C (detected alloy melting point), the wetting experiments were performed by achieving the isothermal conditions with a heating rate of 10 °C/s and the temperature was in real time monitored by a pyrometer (Minolta-CYCLOPS52).

The testing temperature was kept constant for around 15 min and then the sample was quenched (cooling rate 20 °C/s) to preserve the developed interface microstructures.

By an image analysis software ad hoc-developed (ASTRAVIEW®) [25] and connected to a high-resolution CCD-camera, the evolution of contact angles and drop geometric variables (R-base radius and H-drop height) was in real-time followed and recorded.

The same experimental set-up was used for processing the Si-10Zr alloy onto GC at T = 1450 °C by following the above described experimental procedure.

The experimental complex described in details in [26], was used to study the wettability and spreading kinetics in the Si-10Zr/SiC system by squeezing the melted alloy on the substrate at the testing temperature of T = 1450 °C under a static Ar atmosphere.

The presence of Ta as heating element, acting as an oxygen getter, ensures an oxygen partial pressure inside the test chamber that is imposed by thermodynamics of the (4/5) Ta + O$_2$ = (2/5) Ta$_2$O$_5$ reaction
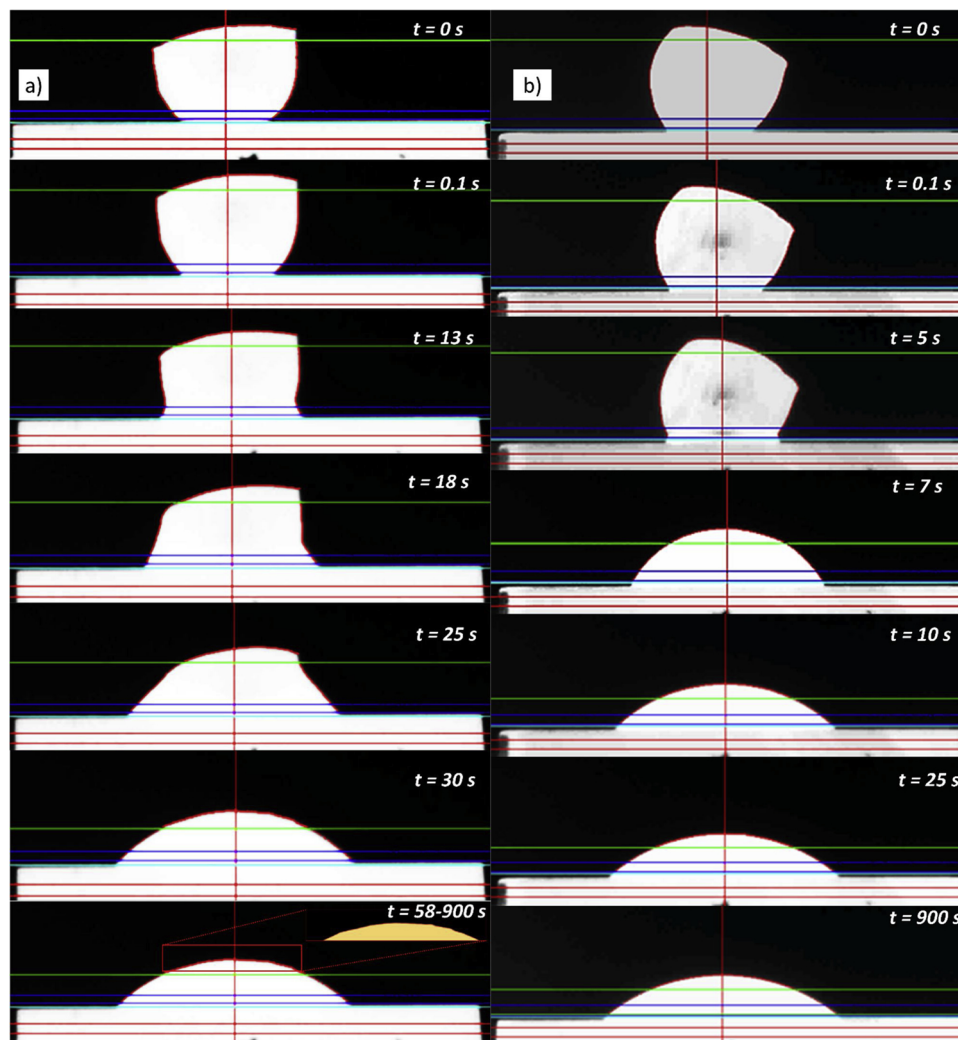
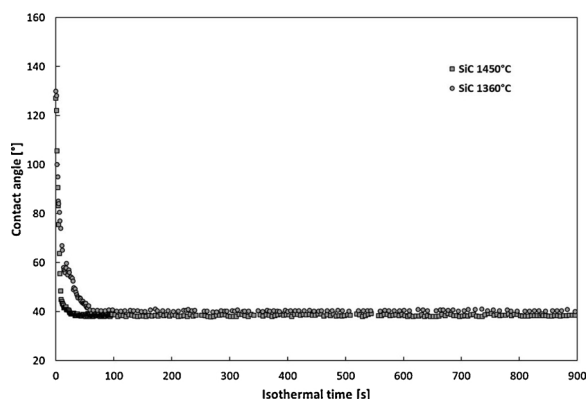**Fig. 2.** Time sequence images recorded during the Si-10Zr spreading on SiC: a) at T = 1360 °C and b) at T = 1450 °C.

Fig. 3. Wettability of the Si-10Zr/SiC couples processed for 15 min under an Ar atmosphere at: (●) T = 1360 °C and (■) T = 1450 °C.

[27]. Accordingly, at the testing temperature of T = 1450 °C, the oxygen partial pressure value of $PO_2 < 10^{-14}$ mbar was obtained.

At the selected testing temperature of T = 1450 °C, the melted alloy was squeezed through the hole (diameter 1 mm) of an Al_2O_3 capillary by a piston and deposited onto the SiC substrate.

Within the alloy squeezing, native oxide layers grown up at room temperature or segregated at the alloy surface, are mechanically broken and removed, thus an oxide-free molten surface is exposed to the

surrounding experimental environment [28]. On the other hand, the liquid free-oxide surface may readily interact with the tip of the capillary and further surface oxidation and evaporation phenomena can be promoted [28,29].

At the end of the isothermal time (t = 15 min) the chamber was cooled from T = 1450 °C down to the room temperature with a rate of 20 °C/min.

Every single frame was processed by ASTRAVIEW® software and the contact angle values, drop geometric parameters were measured to analyze the wettability and spreading behaviours over time.

2.3. Surface and microstructural characterization

After the wetting tests, all the samples were embedded in epoxy-resin, cross-sectioned, metallographically polished and prepared for the microstructural characterization.

As already introduced, in order to analyze the microstructure and reaction products, both at the top and at the cross-sectioned solidified drop, an Optical Microscope (ZEISS) and a Scanning Electron Microscopy (SEM) equipped with an energy dispersive X-Ray detectors (EDS) were used.
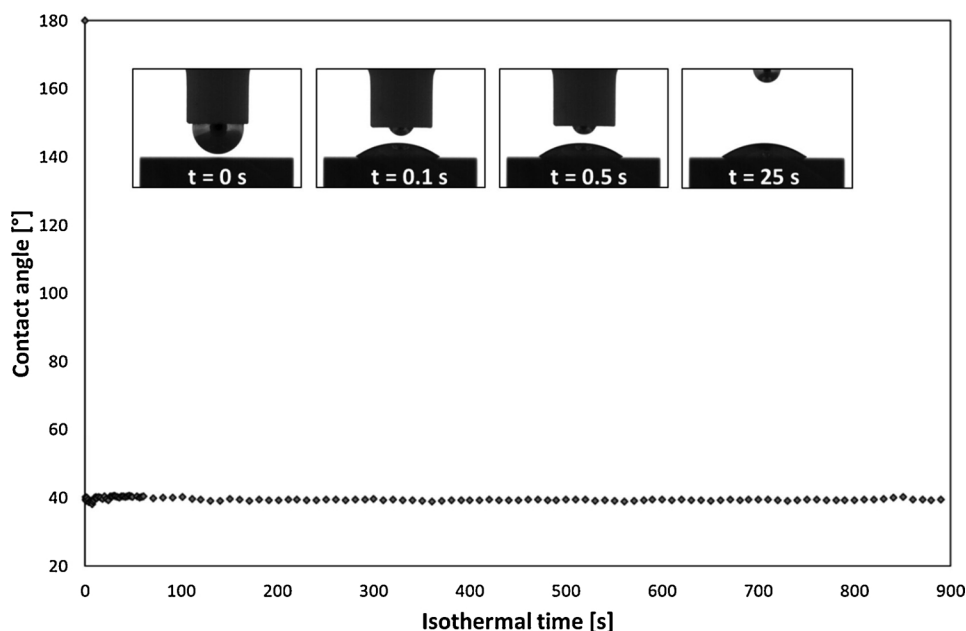
Fig. 4. Contact angle value as a function of time the liquid Si-10Zr/SiC system within the wetting test performed by the dispensed drop at T =1450 °C under an Ar atmosphere.

3. Results and discussion

3.1. Wettability as a function of temperature

In Fig. 2, the time sequences of the Si-10Zr alloy spreading on SiC at the temperatures of T =1360 °C, as detected alloy melting point (Fig. 2a), and T =1450 °C (Fig. 2b), are shown.

Different Si-Zr eutectic compositions in the Si-rich side, as well as a range of 30 °C in the eutectic melting temperature range, are reported in [31–34]. In particular, by analyzing the invariant reactions in the Si-Zr system, the Si-10Zr alloy was determined as Si-Zr eutectic composition with a melting range of 1355.15 ÷ 1370 °C [32].

The detected melting point of the Si-10Zr alloy in contact with SiC at T =1360 °C, is in agreement with the values reported in literature. However, it worth to be mention that a two phase microstructure, typical of hypoeutectic alloys, was revealed by the EDS analyses performed at the as-produced cross-sectioned alloy sample (Fig. 1). In particular, a $ZrSi_2$ phase was rejected during solidification as segregating phase at the surface and even at the bottom of the drop embedded in an eutectic matrix with a Zr-content varying from 8.1–9 at%. It is in agreement with the recent Si-Zr phase diagram calculation reported in [31] and optimized by using newly thermodynamic data as inputs. Consequently, the new calculated Si-Zr eutectic alloy in the Si-rich phase was reassessed at a Zr-content of 8.19 at% and a melting temperature of T =1345.7 °C. Hence, the higher detected melting point can be explained by the presence of embedded high melting point phase ($ZrSi_2$: Tm =1620 °C [30]). It is confirmed by the appearance of a solid phase segregated at the top of the drop (Fig. 2a). Additionally, as it can be evinced by following the sequence of alloy melting and spreading, at T =1360 °C (Fig. 2a), the first evidence of melting is observed at the bottom of the alloy drop and the samples took 30 s and 7 s to achieve the spherical drop shape at T =1360 °C and 1450 °C, respectively.

It is well known that the presence of a SiO_2-native oxide layer at Si and Si-based alloy surfaces, typically revealed during wetting tests performed by the contact heating sessile drop [19,28], may be a competitive phenomenon in delaying the complete melting of the drop [35]. Nevertheless, the native oxide should be decomposed by its reaction with liquid Si, forming the volatile Si-monoxide:

$$SiO_{2(s)} + Si_{(l)} \rightarrow 2SiO_{(g)} \uparrow \qquad (1)$$

When the layer of native oxide completely disappears at the interface, liquid Si interacts with the substrate. The SiO_2 oxide layer can be present also at the SiC surface and similarly, its decomposition is promoted by the same reaction (reaction 1).

Moreover, the following reaction (reaction 2) may be considered in promoting the SiO_2 layer decomposition potentially present at the Si-Zr alloy/SiC interface:

$$2SiO_{2(s)} + SiC_{(s)} \rightarrow CO_{(g)} \uparrow + 3SiO_{(g)} \uparrow \qquad (2)$$
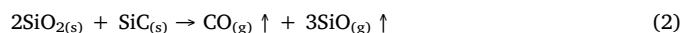
Accordingly, the first evidences of alloy melting are observed at the interface (Fig. 2a and b).

By following the contact angles evolution over time at T =1360 °C and T =1450 °C (Fig. 3), at the lower temperature, the steady state condition is achieved in 58 s and a final contact angle value of θ = 40° was measured. On the contrary, by increasing the temperature up to T =1450 °C, the final value of θ = 38° was reached in around 25 s. Such wetting kinetics as a function of temperature, are typical of non-reactive systems where the adhesion (Van der Walls forces) is the only occurring interfacial phenomenon.

3.2. Sessile drop versus dispensed drop

As aforementioned, to investigate the presence of SiO_2 primary oxide as affecting factor on the spreading kinetics, a wetting experiment was performed by dispensing a liquid Si-10Zr alloy drop trough an Al_2O_3 capillary onto the SiC substrate at T =1450 °C.

On the other hand, the presence of a Si-based alloy surface under oxide-free condition, promotes much more evaporation phenomena [39].

As it can be seen in Fig. 4, by following the evolution of contact angle values and even the inserted time sequence images of the alloy squeezing trough the capillary, although the rate of image recording was 10 frames/s, it was not possible to detect and record exactly the deposition of the melt alloy onto the SiC substrate. In addition, as it can be evinced by the Fig. 4, the alloy drop was placed on the substrate without any other movement of the capillary and piston. Specifically, at a distance of less than 0.5 mm, it seems that the alloy drop detached itself and instantaneously went to wet the substrate. Within the first 5 s after the alloy detachment, a weak perturbation of the contact angle
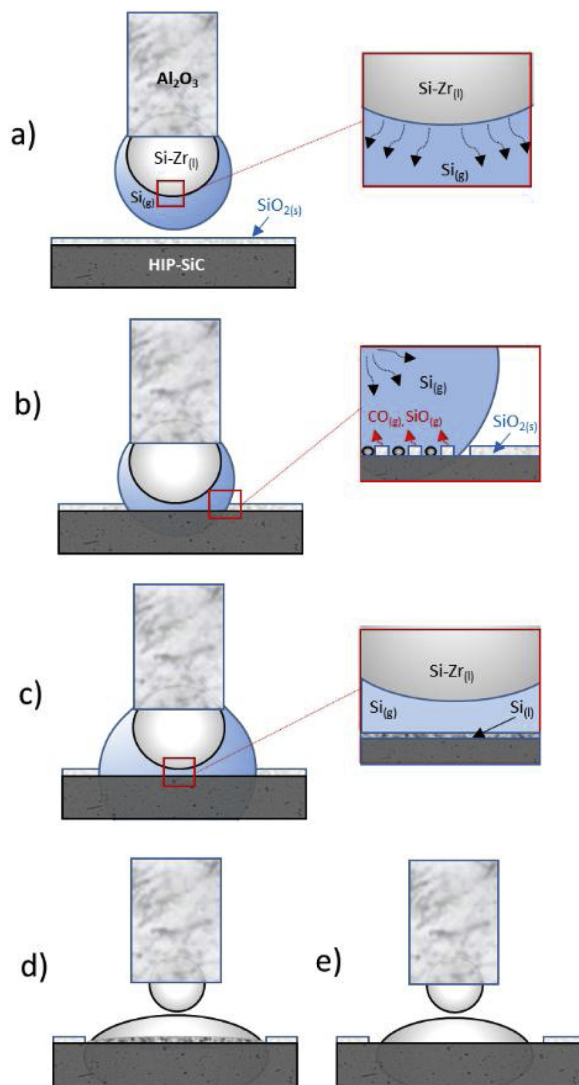
Fig. 5. Scheme of liquid Si-10Zr alloy deposition onto the SiC substrate with highlighted all the possible occurring phenomena.

value was observed.

During the approaching of the capillary to the SiC substrate, taking into account the occurring Si evaporation from the alloy surface, the condensation of Si droplets on the SiC substrate can not be excluded [40], as shown in Fig. 5. The Si droplets condensate at the SiC surface, may rearrange themselves in a liquid Si layer (see Fig. 5b and c) and the

SiO_2-decomposition, according to the reaction 1, can take place. Additionally, at a distance of 0.5 mm, the Si-evaporation and condensation domains were presumably overlapping and consequently favoring the transferring of molten material from the pendant drop to the SiC substrate. At the first instants, the transferred molten material was most probably "wetting" the liquid Si-layer (see Fig. 5d) and forming a Si-10Zr/Si liquid interface which correspons to the minimum of contact angle value observed (see Fig. 4). Furthermore, the conservation of momentum should be considered. After such perturbation, the Si-10Zr/SiC interface achieved suddenly the equilibrium condition which was preserved until the end of the experiment with a measured contact angle value of 39° (see Figs. 4 and 5 e).

The contact angle value of θ = 39° measured for the Si-10Zr alloy drop squeezed on the SiC substrate is in a very good agreement with the final contact angle measured at the same temperature within the contact heating sessile drop experiments, confirming that only the initial stage of spreading was affected by the presence of SiO_2 both at the alloy surface and on the SiC substrate.

Fig. 6 shows the images of the Al_2O_3-capillary and Si-10Zr/SiC sample after the wetting experiment performed by the dispensed drop method. In particular, a crack most probably generated in the capillary during the decrease of temperature, was revealed (Fig. 6a). The crack of the Al_2O_3-capillary, as container of the alloy material, is due to the mismatching in the CTE values of Al_2O_3 and Si-based materials [36]. Moreover, the presence of Zr increases the wettability of Si-based alloys with oxide-based ceramics, mainly at temperature higher than 1400 °C [37]. Additional factor to be taken into account is the anomalous volume expansion exhibited by Si and Si-based alloys during their solidification [38] inducing the typical conical angle at the top of the solidified drop (Fig. 6c).

3.3. Wettability as a function of the substrate: SiC versus GC

In Fig. 7, the wetting behavior observed at T = 1450 °C at the Si-10Zr/GC triple line during the contact heating sessile drop experiment, is shown and compared with the behavior observed in liquid Si-10Zr/SiC system under the same operative conditions. In particular, the transition from non-wetting to wetting behavior for Si-10Zr/GC couple took 17 s (θ < 90°), as shown in Fig. 7b. In fact, within the previous spreading stage, liquid Si reacts exothermically with C as follows:

$$Si_{(l)} + C_{(s)} \rightarrow SiC_{(s)} \tag{3}$$

and the progressively growth of a well-wettable SiC layer at the Si-10Zr/GC interface, is predictable. Moreover, the system achieved the equilibrium contact angle value of 43° in 60 s with a spreading rate lower than the Si-10Zr/SiC couple, as expected. The equilibrium contact angle value measured in the Si-10Zr/GC system is higher than the value shown under the same testing conditions at Si-10Zr/SiC interface
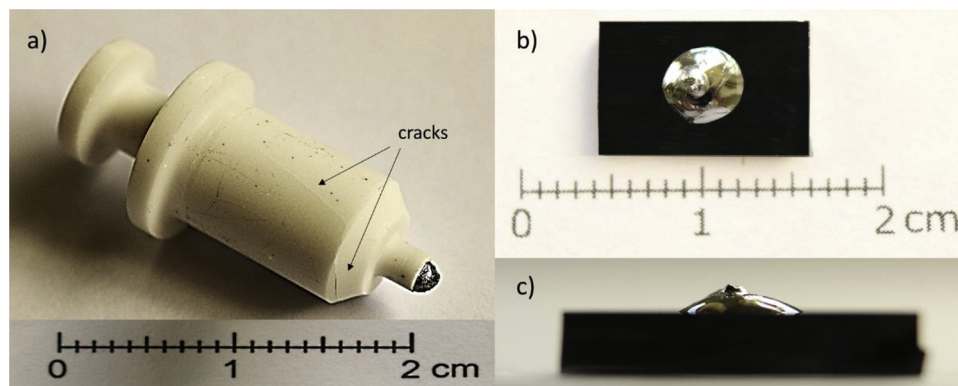

Fig. 6. Photographs of the a) Al_2O_3-capillary and b) top and c) front view of Si-10Zr/SiC sample after the wetting test performed by the dispensed drop method at T = 1450 °C under an Ar atmosphere.
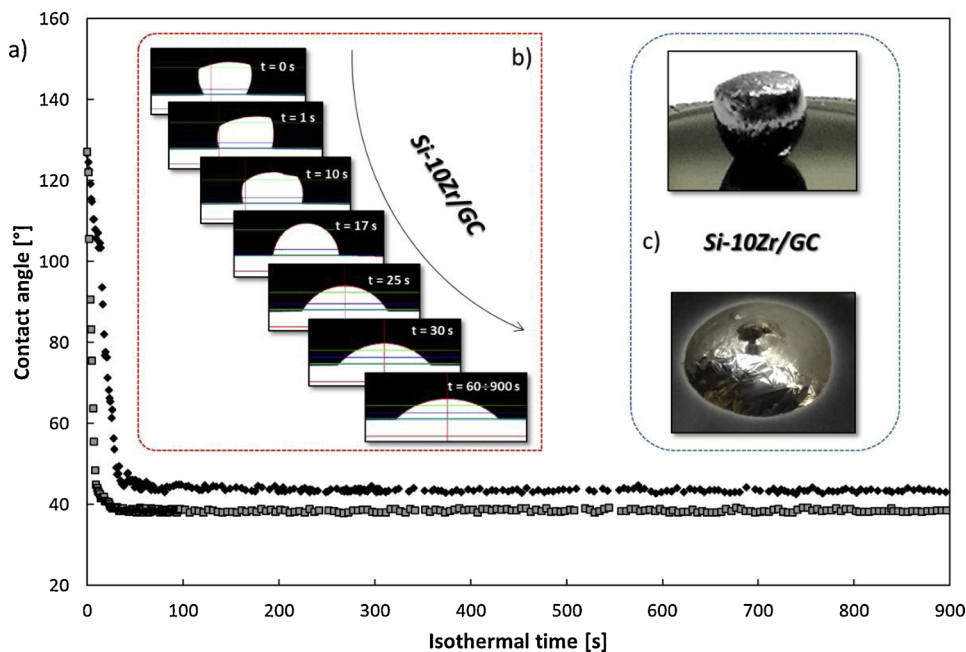
Fig. 7. Wettability of liquid Si-10Zr in contact with GC (◆) and SiC (■) observed at T = 1450 °C and under Ar atmosphere for 15 min: a) contact angle behaviors; b) time sequence of alloy spreading on GC; c) Si-10Zr/GC samples before and after the wetting experiments.
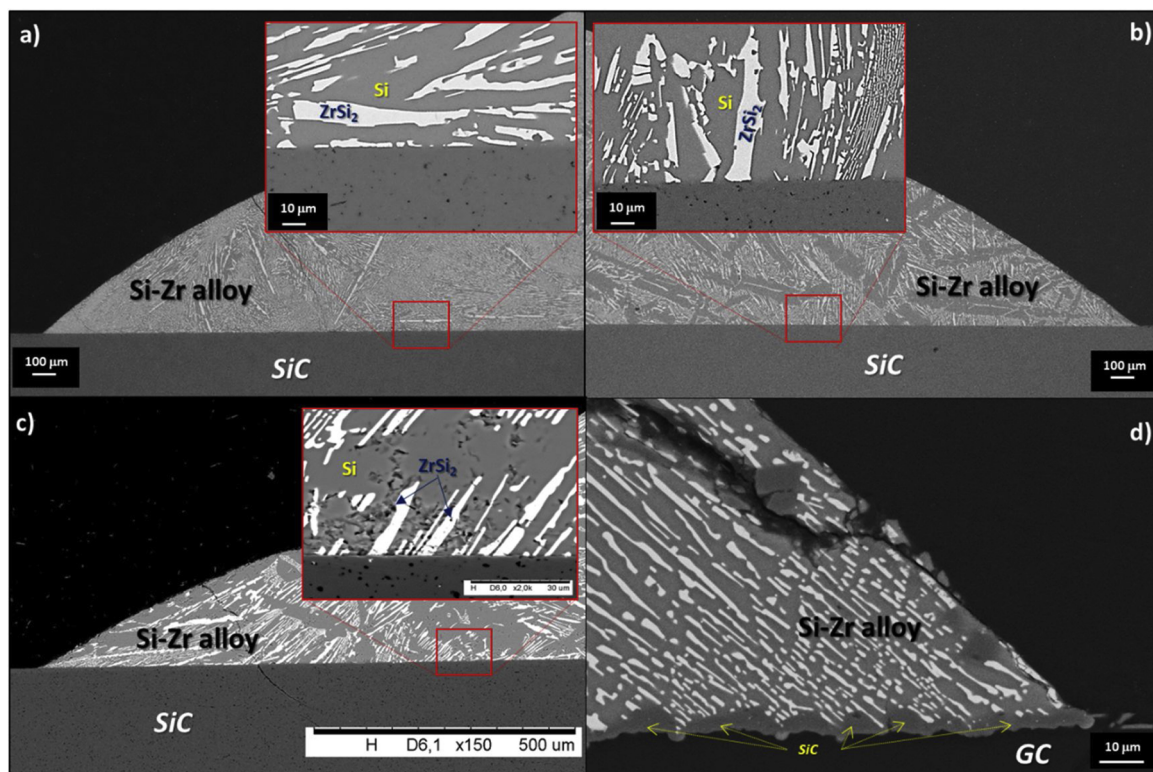

Fig. 8. BSE/EDS analyses performed at different magnifications at the triple lines of Si-10Zr/SiC processed by the sessile drop method a) at T = 1360 °C, b) at T = 1450 °C; c) by the dispensed drop method at T = 1450 °C, and d) Si-10Zr/GC by the sessile drop method at T = 1450 °C.

(θ = 39°). It is given by the rougher Si-10Zr/GC interface developed by the growth of the reaction layer (SiC).

After the wetting experiment (Fig. 7c), a shadow surrounding the drop perimeter was revealed at the triple line, as in the case of other Si-based alloys previously investigated under the same operating conditions [18,19]. In such cases, the Si-evaporation/condensation phenomena, more pronounced at high temperatures, are revealed beyond the triple line by the appearance of a thin SiC-layer which may favours further advancing of the triple line [20,28].

The equilibrium contact angle values observed for the liquid Si-10Zr alloy in contact with SiC and GC as a function of the temperature are in a very good agreement with the values measured by [24] for the liquid Si-8at%Zr in contact with the same substrates over the temperature range of 1400−1500 °C under an Ar atmosphere. In particular, the contact angle values measured at the Si-8at%Zr/SiC interface in the temperature range investigated are comparable with the values reported in this work, taking into account the slight difference in the alloy composition. In contrast, an anomalous trend is described for Si-8at%

Zr/GC system in [24]. Specifically, a contact angle value around 46° is reported during the contact heating of the sample from the detected alloy melting point (T = 1404 °C) to 1452 °C. At T = 1452 °C, the contact angle value sharply decreased to 29° and then remained constant throughout the experiment at 1500 °C. As explained by the authors, the slower initial spreading (in the range of 1404 °C–1452 °C) may be caused by the alloy homogenization and by the reactive process ongoing at the interface resulting in the appearance of a SiC layer as reaction product.

Although evidences are not reported in the paper, another possible explanation given by the authors was the alloy contamination by oxygen.

3.4. Developed microstructures at Si-10Zr/SiC and Si-10Zr/GC interfaces

In Fig. 8, the BSE/EDS analyses performed at the triple lines of Si-10Zr/SiC (Fig. 8a–c) and Si-10Zr/GC (Fig. 8d) samples after the wetting experiments, are shown. In particular, as it can be seen in Fig. 8a and b, the metal phase well adheres at the SiC surface and absence of reaction and SiC-dissolution phenomena are detected both at T = 1360 °C and T = 1450 °C, respectively. Additionally, the alloy drops in contact with the SiC surface exhibit a Si-ZrSi$_2$ two phase microstructure with needle shaped developed ZrSi$_2$ crystals embedded in a Si-matrix. The same occurring interfacial phenomena may control the microstructural development in the Si-10Zr/SiC system processed at T = 1450 °C by the dispensed drop method (Fig. 8c). Contrarily, as a reactive system, the presence of a compacted SiC reaction layer was revealed at the Si-10Zr/GC interface. In particular, SiC crystals epitaxially grown up to a size of 2–5 μm were detected as well as the presence of C-dissolution pockets, as shown in Fig. 8d. The growth of SiC crystals results in the increase of roughness and consequently in a higher value of the "apparent" contact angle (θ = 43°) respect to the value measured at the Si-10Zr/SiC triple line at the same temperature (θ = 38°).

In view to optimize reactive infiltration process and mainly to better understand the pore closure/narrowing phenomena, the reactivity as a function of Si-content is worthy to be investigated, as well as the valuable set of thermophysical properties which can be used as input data for computational simulations.

4. Conclusions

Aiming to develop refractory advanced composite materials such as SiC/ZrSi$_2$ fabricated via reactive infiltration, fundamental studies on the wettability and interfacial phenomena occurring at the liquid Si-10Zr/SiC interface were performed by the contact heating sessile drop method as a function of the temperature under an atmosphere with reduced oxygen content.

Specifically, the interfacial phenomena in terms of contact angle behavior, spreading kinetics, developed microstructures at the interfaces, occurring in the temperature range of 1360 − 1450 °C were widely analyzed, discussed and related to the operating conditions.

The final contact angle values seem weakly affected by the temperature and a very good wettability (perfect adherence) was observed even at the alloy melting point without any dissolution of the SiC substrate.

Such findings provide fruitful know-how for predicting good thermal compatibility and mechanical response of fabricated SiC/ZrSi$_2$ composites via liquid-assisted process such as reactive infiltration.

A careful investigation was also performed at T = 1450 °C to investigate possible affecting factors or technological problems encountered within an infiltration process, such as the presence of SiO$_2$ as native oxide on both the infiltrating material and at the pore walls of the SiC preform, as well as the presence of residual C. For the mentioned reasons, targeted wetting experiments were performed by squeezing the alloy on SiC and by contact heating on GC. In particular, the two different no-reactive and reactive mechanisms controlling the

wettability of the liquid Si-10Zr alloy in contact with SiC and GC, respectively were clearly evinced. Additionally, the growing and thickening of SiC-crystals at the Si-10Zr/GC interface was carefully documented with the aim to provide fruitful indications for better understanding the pore closure/narrowing phenomena affecting the reactive infiltration process.

Declaration of Competing Interest

None.

References

[1] J. Binner, M. Porter, B. Baker, J. Zou, V. Venkatachalam, V.R. Diaz, A. D'Angio, P. Ramanujam, T. Zhang, T.S.R.C. Murthy, Selection, processing, properties and applications of ultra-high temperature ceramic matrix composites, UHTCMCs – a review, Int. Mater. Rev. (2019), https://doi.org/10.1080/09506608.2019.1652006.

[2] S.T. Mileiko, Constituent compatibility and microstructural stability, Compr. Comp. Mater. 4 (2000) 265–287.

[3] A. Siddharth Sharma, P. Fitriani, D.H. Yoon, Fabrication of SiCf/SiC and integrated assemblies for nuclear reactor applications, Ceram. Int. 43 (2017) 17211–17215.

[4] T. Koyanagi, Y. Katoh, T. Nozawa, L.L. Snead, S. Kondo, C.H. Henager Jr., M. Ferraris, T. Hinoki, Q. Huang, Recent progress in the development of SiC composites for nuclear fusion applications, J. Nucl. Mater. 511 (2018) 544–555.

[5] M. Li, X. Zhou, H. Yang, S. Du, Q. Huang, The critical issues of SiC materials for future nuclear systems, Scr. Mater. 143 (2018) 149–153.

[6] Y.G. Tong, Z.H. Cai, S.X. Bai, Y.L. Hu, M.Y. Hua, W. Xie, Y.C. Ye, Y. Li, Microstructures and properties of Si-Zr alloy based CMCs reinforced by various porous C/C performs, Ceram. Int. 44 (2018) 16577–16582.

[7] Z. Zhou, Z. Sun, Yicheng Ge, Ke Peng, Liping Ran, Maozhong Yi, Microstructure and ablation performance of SiC–ZrC coated C/C composites prepared by reactive melt infiltration, Ceram. Int. 44 (2018) 8314–8321.

[8] Y. Katoh, L.L. Snead, C.H. Henager Jr., A. Hasegawa, A. Kohyama, B. Riccardi, H. Hegeman, Current status and critical issues for development of SiC composites for fusion applications, J. Nucl. Mater. 367–370 (2007) 659–671.

[9] O.C. Esteban, M. Caccia, A. Camarano, J. Narciso, Advances in High Temperature Ceramic Matrix Composites and Materials for Sustainable Development; Ceramic Transactions, John Wiley & Sons, 2017.

[10] M. Aronovici, G. Bianchi, L. Ferrari, M. Barbato, S. Gianella, G. Scocchi, A. Ortona, Heat and mass transfer in ceramic lattices during high-temperature oxidation, J. Am. Ceram. Soc. 98 (8) (2015) 2625–2633.

[11] Il-Je Cho, Kyung-Tae Park, Sang-Ki Lee, Hayk H. Nersisyan, Yong-Soo Kim, Jong-Hyeon Lee, Rapid and cost-effective method for synthesizing zirconium silicides, Chem. Eng. J. 165 (2010) 728–734.

[12] M. Le Flem, J. Canel, S. Urvoy, Processing and characterization of Zr3Si2 for nuclear applications, J. Alloys. Compd. 465 (2008) 269–273.

[13] H. Yeom, L. He, R. Mariani, K. Sridharan, Structural evolution of oxidized surface of zirconium-silicide under ion irradiation, Appl. Surf. Sci. 455 (2018) 333–342.

[14] R. Novakovic, D. Giuranno, M. Caccia, S. Amore, R. Nowak, N. Sobczak, J. Narciso, E. Ricci, Thermodynamic, surface and structural properties of liquid Co-Si alloys, J. Mol. Liq. 221 (2016) 346–353.

[15] R. Novakovic, E. Ricci, D. Giuranno, T. Lanata, S. Amore, Thermodynamics and surface properties of liquid Bi-In alloys, Calphad 33 (2009) 69–75.

[16] D. Giuranno, A. Tuissi, R. Novakovic, E. Ricci, Surface tension and density of Al-Ni alloys, J. Chem. Eng. Data 55 (2010) 3024–3028.

[17] S. Amore, D. Giuranno, R. Novakovic, E. Ricci, R. Nowak, N. Sobczak, Thermodynamic and surface properties of liquid Ge-Si alloys, Calphad 44 (2014) 95–101.

[18] D. Giuranno, N. Sobczac, G. Bruzda, R. Nowak, W. Polkowski, A. Kudyba, A. Polkowska, R. Novakovic, Studying the wettability and reactivity of liquid Si-Ti eutectic alloy on glassy carbon, J. Mater. Eng. Perform. 28 (6) (2019) 3460–3467.

[19] D. Giuranno, N. Sobczac, G. Bruzda, R. Nowak, W. Polkowski, A. Kudyba,

A. Polkowska, R. Novakovic, Wetting and spreading behavior of liquid Si-Ti eutectic alloy in contact with glassy carbon and SiC at T = 1450 °C, Metall. Mater. Trans A 50 (10) (2019) 4814–4826.

[20] M. Caccia, S. Amore, D. Giuranno, R. Novakovic, E. Ricci, J. Narciso, Towards optimization of SiC/CoSi$_2$ composite material manufacture via reactive infiltration: wetting study of Si–Co alloys on carbon materials, J. Eur. Ceram. Soc. 35 (15) (2015) 4099–4106.

[21] J. Roger, G. Chollon, Mechanisms and kinetics during reactive infiltration of molten silicon in porous graphite, Ceram. Int. 45 (2019) 8690–8699.

[22] Y. Tong, H. Zhang, X.B. Liang, C.Y. Lee, S.X. Bai, Q.H. Qin, Surface tension calculation of Si-Zr alloys for reactive infiltration of SiC and/or ZrC based ceramic composites, Res. Rev. Mater. Sci. Chem. 6 (2) (2016) 115–130.

[23] B.J. Keene, A review of the surface tension of Silicon and its alloys with reference to Marangoni Flow, Surf. Interface Anal. 10 (1987) 367–383.

[24] M. Naikadea, B. Fankhänel, L. Weber, A. Ortona, M. Stelter, T. Graule, Studying the wettability of Si and eutectic Si-Zr alloy on carbon and silicon carbide by sessile drop experiments, J. Eur. Ceram. Soc. 39 (2019) 735–742.

[25] L. Liggieri, A. Passerone, An automatic technique for measuring the surface tension of liquid metals, High. Technol. 7 (1989) 80–86.

[26] N. Sobczak, R. Nowak, W. Radziwill, J. Budzioch, A. Glenz, Experimental complex for investigations of high temperature capillarity phenomena, Mat. Sci. Eng. A 495 (2008) 43–49.

[27] O. Knacke, O. Kubaschewski, K. Hesselmann, Thermochemical Properties of Inorganic Substances, 2nd ed., Springer Verlag, Düsseldorf, 1991.

[28] B. Drevet, N. Eustathopoulos, Wetting of ceramics by molten silicon and silicon alloys: a review, J. Mater. Sci. 47 (2012) 8247–8260.

[29] N. Eustathopoulos, B. Drevet, Surface tension of liquid silicon: high or low value? J. Crys. Grow. 371 (2013) 77–83.

[30] E. Ricci, D. Giuranno, N. Sobczak, Further development of testing procedures for high temperature surface tension measurements, J. Mater. Eng. Perform. 22 (11) (2013) 3381–3388.

[31] H.M. Chen, F. Zheng, H.S. Liu, L.B. Liu, Z.P. Jin, Thermodynamic assessment of B–Zr and Si–Zr binary systems, J. Alloys. Compd. 468 (2009) 209–216.

[32] H.M. Chen, Y. Xiang, S. Wang, F. Zheng, L.B. Liu, Z.P. Jin, Thermodynamic assessment of the C–Si–Zr system, J. Alloys. Compd. 474 (2009) 76–80.

[33] H. Okamoto, Bull. Alloy Phase Diag. 11 (5) (1990) 513–519.

[34] C. Gueneau, C. Servant, I. Ansara, N. Dupin, Thermodynamic assessment of the Si-Zr system, CALPHAD 18 (3) (1994) 319–327.

[35] N. Eustathopoulos, N. Sobczak, A. Passerone, K. Nogi, Measurement of contact angle and work of adhesion at high temperature, J. Mater. Sci. 40 (2005) 2271–2280.

[36] T. Iida, R.I.L. Guthrie, The Physical Properties of Liquid Metals, Clarendon Press, Oxford, 1993.

[37] R. Novakovic, E. Ricci, M.L. Muolo, D. Giuranno, A. Passerone, On the application of modelling to study the surface and interfacial phenomena in liquid alloy-ceramic substrate systems, Intermetallics 11 (11-12) (2003) 1301–1311.

[38] Truong V. Vu, Quan H. Luu, Containerless solidification of a droplet under forced convection, Int. J. Heat Mass Transf. 143 (2019) 118498.

[39] D. Giuranno, E. Arato, E. Ricci, Oxidation conditions of pure liquid metals and alloys, Chem. Eng. Trans. 24 (2011) 571–576.

[40] M. Ratto, E. Ricci, E. Arato, Mechanism of oxidation/deoxidation of liquid silicon: theoretical analysis and interpretation of experimental surface tension data, J. Cryst. Growth 217 (3) (2000) 233–249.